Journal of
Materials Chemistry C

Accepted Manuscript

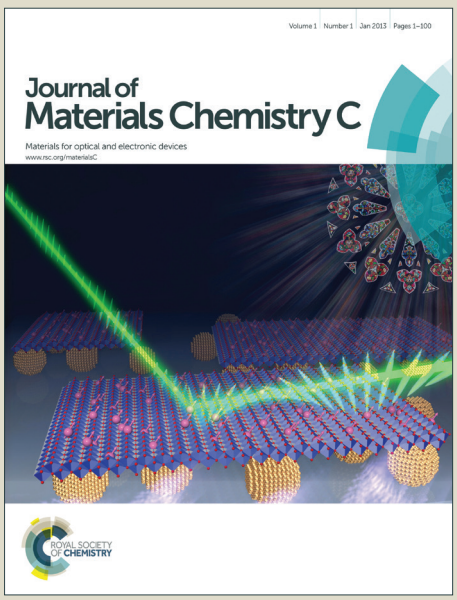

This is an *Accepted Manuscript*, which has been through the Royal Society of Chemistry peer review process and has been accepted for publication.

Accepted Manuscripts are published online shortly after acceptance, before technical editing, formatting and proof reading. Using this free service, authors can make their results available to the community, in citable form, before we publish the edited article. We will replace this *Accepted Manuscript* with the edited and formatted *Advance Article* as soon as it is available.

You can find more information about *Accepted Manuscripts* in the Information for Authors.

Please note that technical editing may introduce minor changes to the text and/or graphics, which may alter content. The journal's standard Terms & Conditions and the Ethical guidelines still apply. In no event shall the Royal Society of Chemistry be held responsible for any errors or omissions in this *Accepted Manuscript* or any consequences arising from the use of any information it contains.

ROYAL SOCIETY OF CHEMISTRY

www.rsc.org/materialsC

Please do not adjust margins

Journal Name

ARTICLE

High performance *n*-type bismuth telluride based alloys for mid-temperature power generation

Received 00th January 20xx,
Accepted 00th January 20xx

DOI: 10.1039/x0xx00000x

www.rsc.org/

Zhenglong Tang,[a] Lipeng Hu,[a] and Tiejun Zhu,*[a,b] Xiaohua Liu,[a] Xinbing Zhao*[a,b]

Currently more than 60% of primary energy used in industry or life is lost as waste heat in the temperature range of 400 ~ 900 K, and more and more attention are paid to mid-temperature thermoelectric (TE) power generation. Here we combine several strategies, i.e. alloying, doping and hot deformation, to improve the TE performance of n-type bismuth telluride based TE alloys for mid-temperature power generation. Se alloying was adopted to widen the band gap and suppress intrinsic conduction at elevated temperatures. When Se atoms completely substitute the Te$^{(2)}$ atoms, the crystal structure of Bi_2Te_3 based alloys tends to be more ordered, resulting in the maximum value of band gap. And the induced alloying scattering significantly reduces the lattice thermal conductivity. Then SbI_3 donor doping was used to increase the electron concentration to further suppress the detrimental effects of bipolar conduction. Finally we applied repetitive hot deformations to further improve the figure of merit *zT* and a peak *zT* of ~1.1 was obtained at about 600 K in the 0.1 at.% SbI_3-$Bi_2Te_{1.9}Se_{1.1}$ alloy, which was hot-deformed three times. The results demonstrated the great potential of the alloy for application in mid-temperature TE power generation .

1. Introduction

Currently more than 60% of primary energy used in industry or life is lost as waste heat in the temperature range of 400 ~ 900 K. And due to the difficulties in heat collection, high cost and some technological issues, much of the waste heat is rarely recovered[1,2]. Thermoelectric (TE) technology, which can realize the direct conversion between heat and electricity, is promising to tackle these issues. The conversion efficiency of a TE device can be measured by the dimensionless figure of merit $zT = \alpha^2\sigma T/\kappa$, where α is the Seebeck coefficient, σ the electrical conductivity, T the operating temperature, and κ the total thermal conductivity (including the lattice contribution κ_{ph}, the carrier contribution κ_{el}, and the ambipolar contribution κ_{amb}), respectively[3,4].

Reviewing the primary TE materials that can be used for power generation, such as PbTe[5-7], half-Heusler alloys[8,9], filled skutterudites[10], $Mg_2Si_{1-x}Sn_x$[11-13], and SnSe[14], their optimal service temperatures mainly reside in the range 650–900 K. However, in the temperature range of 500K-650K, few TE materials are reported to exhibit excellent performance[15-17]. Such an application gap has imposed a pressing demand for high-efficiency TE materials operating in the range 500–650K.

Bismuth telluride (Bi_2Te_3) based bulk materials have been the best commercial TE materials with high *zT* values of ~ 1 near room temperature, and are mainly used in the solid state refrigeration[18]. With the demands on waste heat recovery, Bi_2Te_3 based compounds, $(Bi,Sb)_2(Te,Se)_3$, have recently attracted increasing interest in low temperature power generation applications[19-27]. Hu *et al* reported a high *zT* of ~ 1.3 at 380K for *p*-type polycrystalline $Bi_{0.3}Sb_{1.7}Te_3$ alloys[20] and a figure of merit *zT* ~ 1.2 at 445 K for *n*-type polycrystalline $Bi_2Te_{2.3}Se_{0.7}$ alloys applied for low-temperature power generation[21], the similar results have been achieved by other research groups in recent years[28]. Meanwhile, Wang *et al* reported that the highest *zT* value of *n*-type zone-melted $Bi_2Te_{1.5}Se_{1.5}$ doped with I doping reached 0.86 at 600K, whose average *zT* between 400K and 600K is 0.8[29], Liu *et al* also reported a systematic study on the Bi_2Te_3-Bi_2Se_3-Bi_2S_3 system, found out that *n*-type Bi_2Te_2S showed a peak *zT* ~ 0.8 at 573K and Bi_2SeS_2 ~0.8 at 773K fabricated by high energy ball milling followed by hot pressing[30]. However, in the temperature range of 500-650K, the present property of *n*-type is not high enough to match *p*-type counterparts which had a peak *zT* ~ 0.92 at 710K reported by Hu at al[31]. So it is in crying needs to develop a kind of n-type high-performance TE materials for mid-temperature power generation.

When the Bismuth telluride (Bi_2Te_3) based compounds are applied to mid-temperature power generation, intrinsic excitation becomes the major limitation. The practical solution to suppressing bipolar conduction is to increase the band gap or majority concentration[20]. To widen the band gap, Se alloying can be adopted. The band gap of Bi_2Te_3 is 0.15eV, and Bi_2Se_3 0.35eV, so replacing Te with Se can enlarge band gap, which have been proved by predecessors[32,33]. In addition, Se alloying can introduce much lattice disorder to reduce the

[a]*State Key Laboratory of Silicon Materials, Department of Materials Science and Engineering, Zhejiang University, Hangzhou, China, 310027. E-mail: zhutj@zju.edu.cn; zhaoxb@zju.edu.cn; Fax: +86-571-87951451; Tel: +86-571-87951451*
[b]*Cyrus Tang Center for Sensor Materials and Applications, Zhejiang University, Hangzhou, China, 310027*

Journal of Materials Chemistry C Accepted Manuscript

Please do not adjust margins

κ_{ph}. On the other hand, SbI_3 is generally used as a donor dopant to increase the majority concentration and improve the TE performance [34].

In our previous work, Hu at al. demonstrated that repetitively hot-deformed $Bi_2Te_{2.3}Se_{0.7}$ alloys with engineered intrinsic point defects show the best *zT* in the temperature range 400–500 K[21]. In order to further optimize the band gap of n-type Bi_2Te_3 based compounds for application in higher temperatures, in this paper, we fabricate a series of n-type hot-deformed $Bi_2Te_{3-x}Se_x$ (*x*=0.9-1.4) polycrystalline solid solutions with higher Se contents by a powder metallurgy process, including melting, ball milling (BM), hot pressing (HP) and subsequent hot deformation (HD). The effects of Se alloying on the suppression of intrinsic conduction and the increase of *zT* are systematically investigated. The peak *zT* is shifted above 500 K as a result of band gap widening. Further increasing the carrier concentration by SbI_3 doping, the *zT* peak can be pushed to 600 K. A maximum *zT* ~1.1 at 600 K is obtained by repetitive hot deformation, demonstrating the potential of Bi_2Te_3 based compounds with high Se contents for power generation in 500-650K.

2. Experimental

2.1 Melting

Commercial high-purity elemental chunks of 99.999% Bi, 99.999% Te, and 99.999% Se were used as raw materials. Appropriate quantities of each were weighed according to the nominal compositions of *n*-type $Bi_2Te_{3-x}Se_x$ (x = 0.9-1.4) and sealed into a quartz tube at 10^{-3} Pa. The elemental mixtures were subsequently melted at 1073K for 10 h in a rocking furnace to ensure the composition homogeneity, and then cooled in the furnace to room temperature.

2.2 Consolidation of powders, hot press and hot deformation

Ingots were ball-milled (MM 200, Retsch Gmbh, Haan, Germany) for 20 min at 20 Hz to yield fine powers. These powders were hot pressed into cylindrical shapes in a 10 mm graphite die at 673 K for 30 min under the uniaxial stress of 80 MPa, resulting in a cylinder bulk with a height of 2 mm. The initial hot-pressed bulk samples with different Se content x were named as HP-$Bi_2Te_{3-x}Se_x$(x=0.9-1.4). Subsequently, hot deformation (HD) was performed by repressing the HP samples in a larger graphite die with an inner diameter of 16, 20, and 25 mm each time at 823K for 30 min at the same pressure, named HD-$Bi_2Te_{3-x}Se_x$(x=0.9-1.4). The doping samples were called HD-$y$$SbI_3$+$Bi_2Te_{3-x}Se_x$ (y=0.0005, 0.001, 0.0015, 0.002). This repetitive HD samples were finally named as HD_n-ySbI_3+$Bi_2Te_{3-x}Se_x$ (*n*=1; 2; 3).

2.3 Materials characterization

The phase structure of the samples was investigated by X-ray powder diffraction (XRD) on a Rigaku D/MAX-2550P diffract meter. The in-plane electrical conductivity σ and the Seebeek coefficient α were simultaneously measured on a commercial Linseis® LSR-3 system. The in-plane thermal diffusivity *D* measurement was performed on a Netzsch LFA 457 laser flash apparatus with a Pyroceram standard using the scheme introduced by Xie et al[35]. The specific heat C_P was measured on the Netzsch DSC 404C and the density ρ_D was estimated by an ordinary dimension and weight measurement procedure. The in-plane thermal conductivity was then calculated using the relation $\kappa = D\rho_D C_P$. The Hall coefficient R_H was determined at 300 K on a Quantum Design PPMS-9T instrument using a four-probe configuration. The carrier concentration n_H and in-plane Hall mobility μ_H were calculated according to $n_H = 1/eR_H$ and $\mu_H = \sigma R_H$, respectively, so that the absolute error is on the order of 5%.

3. Results and discussion

3.1 Effects of Se alloying on TE properties of $Bi_2Te_{3-x}Se_x$

3.1.1 Microstructure evolution

The phase structure of the HD-$Bi_2Te_{3-x}Se_x$ compounds was characterized by XRD, as shown in Fig. 1. It is clear that all the diffraction patterns can be indexed to be hexagonal Bi_2Te_2Se (JCPDS#29-0247). All the peaks shift towards higher degrees with the increase of Se content, indicating the formation of $Bi_2Te_{3-x}Se_x$ solid solutions. To investigate the texture degree, the orientation factor *F* of (00l)-planes for the HP and repetitive HD samples was calculated according to the Lotgering method[36]. The *F* value of 0.15 suggests that certain degree preferred orientation is formed in the HP samples, according to the result of *F* values found for n-type samples by Zhao at al. and Shen at al.[28,37]. The higher *F* values of 0.3~0.5 for HD samples characterize their stronger anisotropy. The enhanced texture in HD samples can also be observed in the SEM results, as shown in Fig.2. It is shown that after hot deformation at 823K, the grain size grows and preferential orientation is formed in the HD samples. The anisotropy has to be taken into consideration for textured samples when *zT* values are calculated, as our previous studies indicated that an *F* value of 0.31 could overestimate the *zT* up to 60%[24,38].

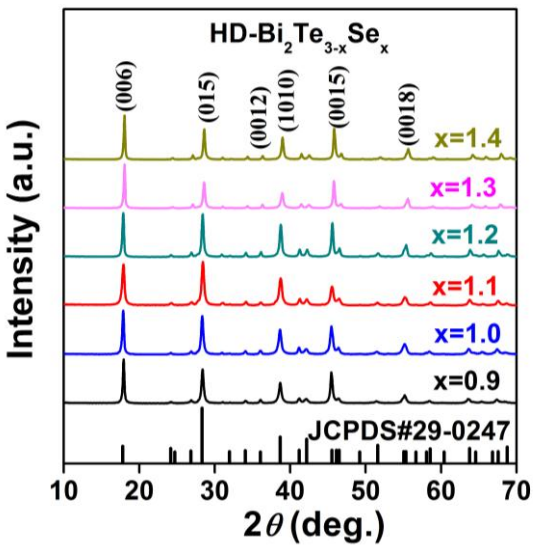

Fig. 1 In-plane XRD patterns of the hot-deformed $Bi_2Te_{3-x}Se_x$ bulk samples (x =0.9-1.4), taken on the hot-deformed surfaces.

This journal is © The Royal Society of Chemistry 20xx
Journal of Materials Chemistry C Accepted Manuscript

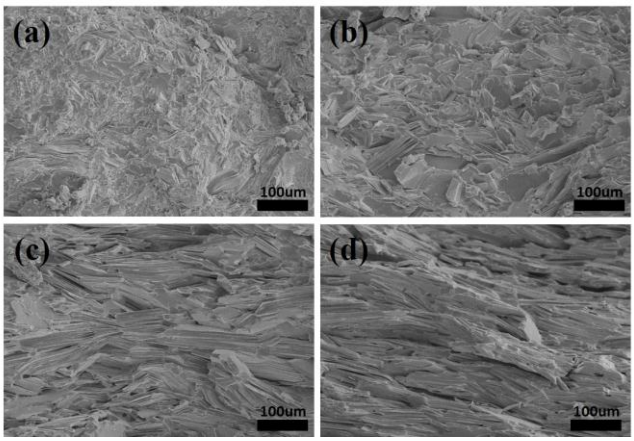

Fig. 2 SEM fractographs of the cross-sections parallel to the pressing direction for the bulk samples before (a) and after hot deformation for once (b), twice (c), and three times (d).

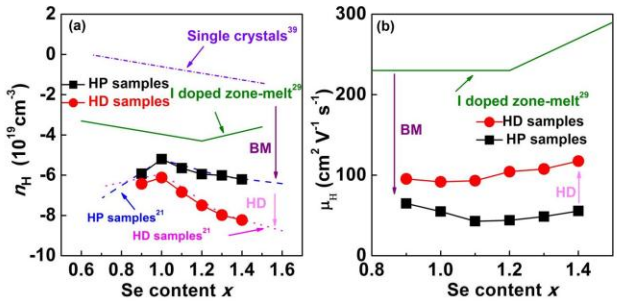

Fig. 3 (a) Se-content dependence of electron concentration (n_H) of hot pressed, hot-deformed $Bi_2Te_{3-x}Se_x$ bulk samples, together with the undoped single crystal[39] and I doped zone-melt samples[29]. (b) Se-content dependence of carrier mobility (u_H) of hot-pressed, hot-deformed $Bi_2Te_{3-x}Se_x$ bulk samples, together with I doped zone-melt samples[29].

3.1.2 Carrier transport

Fig. 3a shows the room temperature carrier concentration n_H of polycrystalline $Bi_2Te_{3-x}Se_x$ samples, together with undoped single crystal[39] and I doped zone-melted crystal[29]. Our samples were obtained by ball milling (BM), hot pressing (HP) and hot deformation (HD). Because of donor-like effect introduced by mechanical deformation[40], all the polycrystalline samples subject to BM (HP and HD samples) show high electron concentrations than single crystal and doped zone-melted crystal. Meanwhile, HD samples show the higher electron concentrations than HP counterparts because hot deformation process also induces donor-like effect[41]. The n_H of polycrystalline HD and HP samples firstly falls and then rises with increasing Se content, which is the result of donor-like effect combined with point defects. The similar phenomenon has also been observed in previous report, and shows a great consistency in the Se content of 0.5-1.5[21,42,43]. While this work focuses on mid-temperature use rather than to achieve the highest zT[21] of n-type Bi_2Te_3 based materials. So we further refine the content gradient to find out the content with largest band gap for higher temperature use. The electron concentration of the samples results from both inherent anon vacancies and deformation-induced donor-like effect. The inherent electron concentration keeps increasing with x, meanwhile the donor-like effect becomes weaker as a result of the lack of the antisite defects concentration when x <1. However, the antisite defects concentration begins to increase when x>1, which causes the re-enhanced donor-like effect leading the increase of the electron concentration[21].

Fig. 3b shows the room temperature carrier mobility u_H of polycrystalline $Bi_2Te_{3-x}Se_x$ samples, together with I doped zone-melted ingot. We can see that the u_H of polycrystalline samples are much smaller than the zone-melted one, as a result of that polycrystalline samples have weaker texture and finer grain sizes that scatter carriers more seriously. Compared with HP samples, the u_H of HD counterparts is larger, as a result of texture enhancement and grain growth, although the latter has the higher carrier concentration[21, 22, 28].

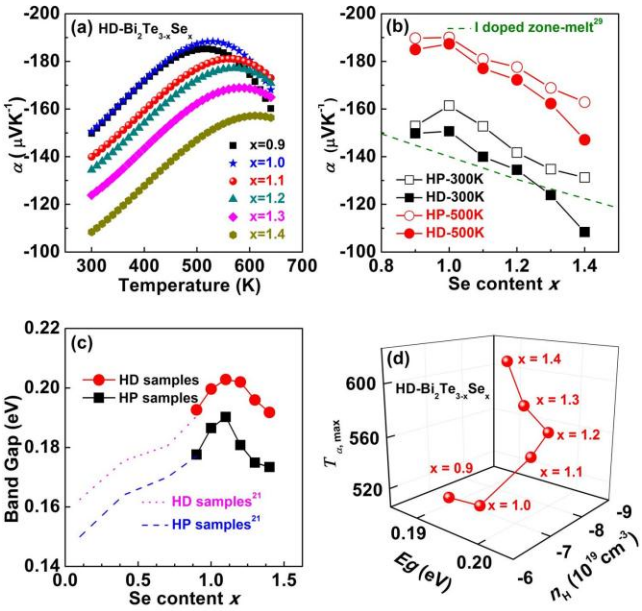

Fig. 4 (a) Temperature dependence of Seebeck coefficient of the hot deformed $Bi_2Te_{3-x}Se_x$ samples. (b) Room temperature and 500 K Seebeck coefficients of the single crystals, HP and HD $Bi_2Te_{3-x}Se_x$ samples. (c) Se-content dependence of band gap of the hot-deformed $Bi_2Te_{3-x}Se_x$ bulk samples. (d) Band gap and electron concentration dependence of temperature when the peak occurs of the hot deformed $Bi_2Te_{3-x}Se_x$ bulk samples.

3.1.3 Seebeck coefficients and band gap

Fig. 4a and b show that the absolute α of polycrystalline HP and HD samples first slightly rises and then falls with increasing x (0.9-1.4), corresponding to the change in n_H in Fig. 3a. Meanwhile, absolute α of HD samples are smaller than HP counterparts both at 300 K and 500 K as a result of donor-like effect induced carrier concentration increase[21,22].

In order to examine the effects of Se alloying on the band gap of $Bi_2Te_{3-x}Se_x$ samples, the band gap of both HP and HD samples was estimated by the relationship $Eg = 2e\alpha_{max}T_{max}$, where α_{max} is the peak Seebeck coefficient and T_{max} the corresponding temperature[20]. As displayed in Fig. 4c, it is shown the band gap first increases and then falls down with increasing Se content x between 0.9-1.4 and it reaches maximum when x=1.1. It is reported that the presence of a maximum and a minimum in energy gap results from the two different types of Te layers in the Bi_2Te_3 structure[44,45]. For single crystals, band gap of Bi_2Te_3 alloyed with Se is found to enlarge with the increase of Se content x, and when x reaches around 1, the band gap goes to its maximum value.[46] Then the

Journal of Materials Chemistry C Accepted Manuscript

band gap begins to decrease with increasing x from 1. In current work, band gap shows a peak at around x=1.1 for the hot-deformed polycrystalline materials and the variation of band gap with Se content agrees well with the results in literature[47].

In Fig.4d, it is worth noting that the temperature of maximum α is pushed to higher temperature with Se alloying although the band gap decreases at x>1.1, mainly due to the increased concentration of majority. As above mentioned, the majority increases with increasing Se content, which can offset the influence of the decrease of band gap at x>1.1.

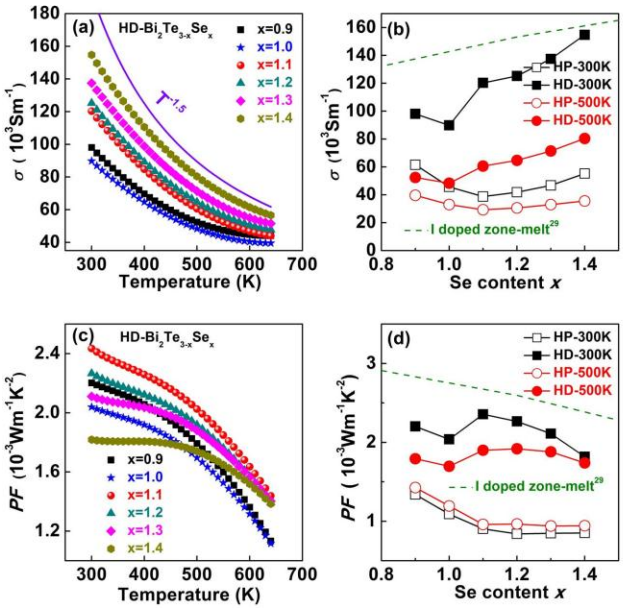

Fig. 5 (a) Temperature dependence of in-plane electrical conductivity of the hot deformed $Bi_2Te_{3-x}Se_x$ samples.(b) Room temperature and 500 K electrical conductivity of the single crystals, HP and HD Bi2Te3-xSex samples. (c) Temperature dependence of power factor of the hot deformed Bi2Te3-xSex samples. (d) Room temperature and 500 K power factor of the single crystals, HP and HD Bi2Te3-xSex samples.

3.1.4 Electrical transport properties

Fig.5a and b show temperature and Se content dependence of in-plane electrical conductivity of $Bi_2Te_{3-x}Se_x$ samples, respectively. The in-plane electrical conductivity σ of HD samples decreases with measurement temperature, indicative of metal-like conduction behavior. The σ firstly decreases then increases with increasing x, consistent with the Se content dependence of carrier concentration. The HD samples exhibit the higher σ than HP counterparts for the studied range of Se content due to the higher μ_H and n_H of the former(Fig.3a, b).

From Fig.5c and d, it is found that HD samples have higher PF for all the compositions compared to HP counterparts due to the remarkably increased σ, consistent with our previous report[21, 22, and 28]. The maximum PF of ~ $2.4\times10^{-3}Wm^{-1}K^{-2}$ is obtained for HD sample at x=1.1 at 300K and stays ~2.0 at 500K.

3.1.5 Thermal conductivity and zT

Fig. 6a, b shows that Se alloying also has an obvious influence on κ. The κ of polycrystalline $Bi_2Te_{3-x}Se_x$ samples firstly drops and then rises with increasing x in accordance with the variation of σ (Fig.5a, b). It can be understood because the contribution of κ_{el} is higher when σ is larger. In the same way, the HD counterparts show higher κ compared with the HP samples. The κ_{ph} of HD samples in Fig. 6c, d was estimated by subtracting the κ_{el} from the total κ, where the κ_{el} was calculated using the Wiedemann-Franz law with L_0 = 2.0×10^{-8} V^2K^{-2}. The κ_{ph} of HD samples keep decreased with increasing Se content, and are lower than that of the HP counterparts. As previously studied[20, 21], multiscale microstructure effects play important roles in the reduced κ_{ph} in polycrystalline HD $Bi_2Te_{3-x}Se_x$ samples. Both antisite defects and vacancies behave as phonon scattering centers and vacancies show stronger scattering on phonon because of the larger mass differences and stress field fluctuations between the occupied sites and the vacancies. During deformation process, a large number of vacancies V_{Bi}''' and $V_{Te}^{\bullet\bullet}$ (or $V_{Se}^{\bullet\bullet}$), and the high-density lattice distortions and dislocations are generated. All of these multiscale defects can effectively scatter phonon to reduce κ_{ph}[21,31].

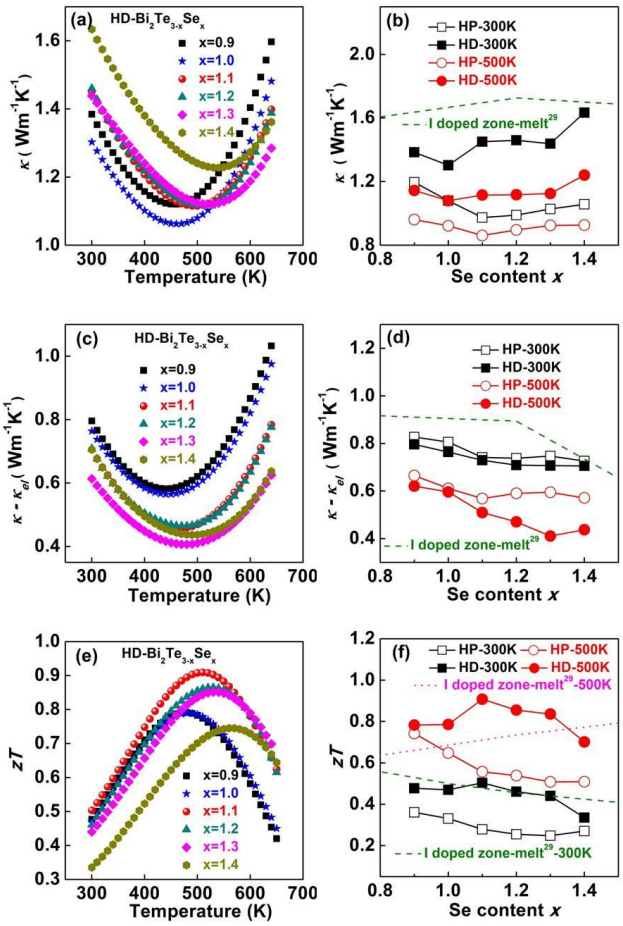

Fig. 6 (a) Temperature dependence of in-plane thermal conductivity of the hot deformed $Bi_2Te_{3-x}Se_x$ samples, (b) Room temperature and 500 K thermal conductivity of the single crystals, HP and HD $Bi_2Te_{3-x}Se_x$ samples, (c) Temperature dependence of in-plane lattice thermal conductivity of the hot deformed $Bi_2Te_{3-x}Se_x$ samples, and (d) Room temperature and 500 K lattice thermal conductivity of the single crystals, HP and HD $Bi_2Te_{3-x}Se_x$ samples. (e) Temperature dependence of in-plane zT of the hot deformed $Bi_2Te_{3-x}Se_x$ samples, (f) Room temperature and 500 K zT of the single crystals, HP and HD $Bi_2Te_{3-x}Se_x$ samples.

The dimensionless figure of merit zT of the HD $Bi_2Te_{3-x}Se_x$ samples is presented in Fig.6e, f with both electrical and thermal properties measured along the in-plane direction. All

Journal of Materials Chemistry C Accepted Manuscript

This journal is © The Royal Society of Chemistry 20xx

the samples with x>1 exhibit a considerable enhancement in zT at higher temperatures compared to the x<1 compounds, especially above 500 K. The highest zT ~ 0.9 at 510K was obtained in $Bi_2Te_{1.9}Se_{1.1}$ HD sample. Although the PF of doped zone-melt samples are higher than polycrystalline counterparts (Fig.5d), the final zT at 500K of HD samples are higher than that of doped zone-melt counterparts, as showed in Fig.6f, as a result of reduced κ_{ph} (Fig.6b). So the HD samples are a better choice used for mid-temperature than doped zone-melt counterparts.

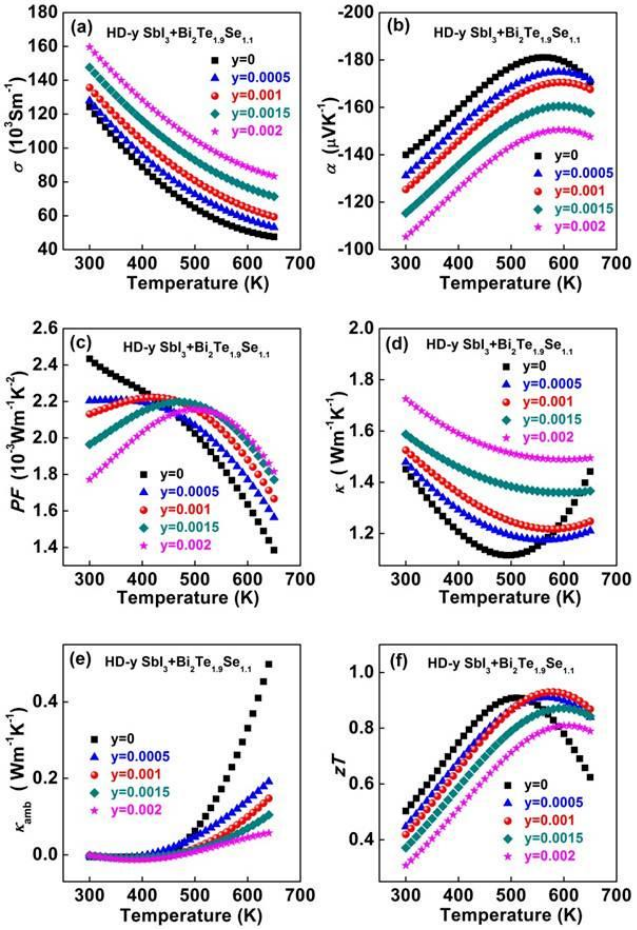

Fig. 7 Temperature dependence of in-plane electrical conductivity (a), Seebeck coefficient (b), power factor (c), in-plane thermal conductivity (d), in-plane ambipolar thermal conductivity (e), and the in-plane zT (f) of the hot-deformed $ySbI_3$-$Bi_2Te_{1.9}Se_{1.1}$ samples.

3.2 Further optimization by SbI_3 doping

Above discussion has demonstrated that Se alloying can widen the band gap and suppress the intrinsic conduction. The temperature for peak zT has been raised to 530K (x=1.1) from 445K (x=0.7) However, the ambipolar diffusion is still serious above 500 K (Fig. 6a and c). We aim at improving the service temperature to 600 K. In the following part, the bipolar conduction above 500 K is expected to be suppressed by increasing the carrier concentration through SbI_3 doping in HD-$Bi_2Te_{1.9}Se_{1.1}$ sample. The carrier concentration increases with the SbI_3 doping content (Fig.S2) The electrical conductivity increases with the doping content, as shown in Fig.7a. Although the Seebeck show the certain decrease with doping, the temperature that α_{max} occurs is increased from 540 K to 590 K at higher doping concentration in Fig 7b. From Fig 7c, the PF of doped samples are higher above about 420K.

In view of the thermal conductivity, it is clear that the minimum values for each samples has been pushed to higher temperatures with increasing SbI_3 content. We evaluated the ambipolar contribution κ_{amb} for the alloys of different SbI_3 content using the method introduced in Ref. 20. It is shown that the contribution of κ_{amb} to the total thermal conductivity is quite large when the carrier concentration is low, especially at high temperatures. With increasing carrier concentration, the ambipolar effects have been greatly reduced. κ_{amb} of pristine sample takes over 50 % of κ at 600 K while the sample y=0.001 only holds 8.3%. Hence, the suppression of ambipolar diffusion significantly contributes to the high zT of ~0.95 at 580 K for HD-0.001SbI_3+$Bi_2Te_{1.9}Se_{1.1}$ sample, compared to HD-$Bi_2Te_{1.9}Se_{1.1}$ counterpart of 0.9 at 510 K.

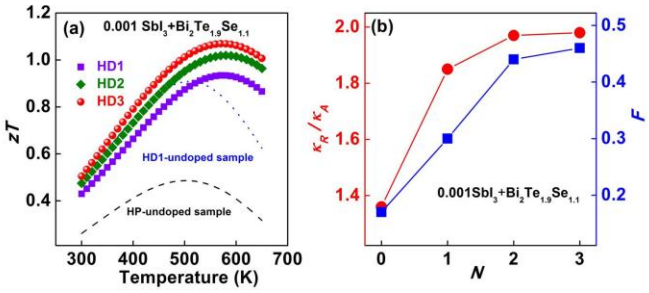

Fig. 8 (a) Temperature dependence of in-plane zT of the repetitive hot-deformed 0.001SbI_3-$Bi_2Te_{1.9}Se_{1.1}$. (b) Thermal transport properties for the $Bi_2Te_2Se_{1.1}$ bulk samples before and after different hot-deformation numbers: κ_R/κ_A and F samples.

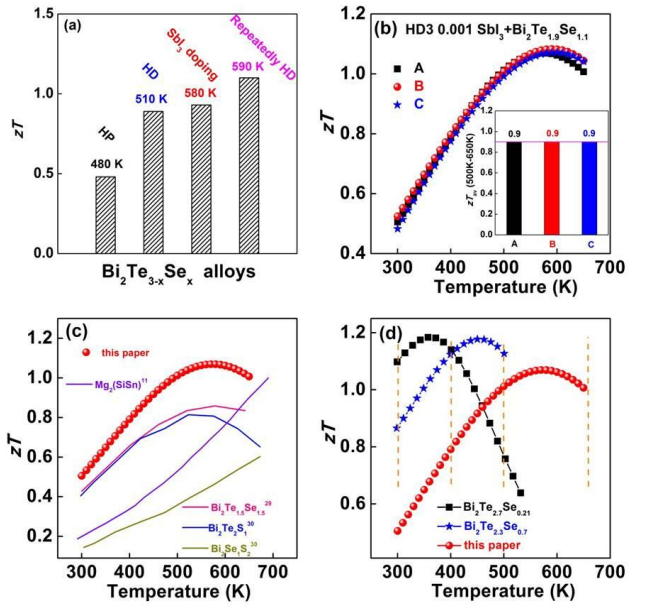

Fig. 9 (a) zT advances of the mid-temperature n-type $Bi_2Te_{3-x}Se_x$-based alloys, (b) Temperature dependence of zT values for the re-prepared HD3-0.001SbI_3-$Bi_2Te_{1.9}Se_{1.1}$ bulk samples, (c) Temperature dependence of zT values of the n-type TE materials applied in mid-temperature ranges, (d) Temperature dependence of zT values of the n-type bismuth telluride compounds applied in different temperature ranges.

3.3 Enhancing the zT by repetitive hot deformation

It has been reported that repetitive hot deformation can effectively improve the TE performance for n-type bismuth

Journal of Materials Chemistry C Accepted Manuscript

telluride based alloys through enhanced texture and increased carrier concentration[21,22]. In this work Fig 8a shows that the optimal $0.001SbI_3+Bi_2Te_{1.9}Se_{1.1}$ sample hot deformed triple has highest *zT* values of ~1.1 at 590K. Fig 8b shows that the texture degree was greatly enhanced by repetitive hot deformations, resulting that the *F* and (κ_R/κ_A) value are getting larger with the increase HD times, which must be taken into consideration in measuring TE parameters for the *zT* calculation to avoid a overestimation, as demonstrated in previous work[28,37].

Fig. 9a shows the *zT* improvement of *n*-type $Bi_2Te_{3-x}Se_x$-based alloys in this work. The *zT* values have been successfully increased from 0.45 to 1.1 and the optimal service temperature has been improved from 480 K to 590 K through Se alloying, optimizing doping and repetitive hot deformation.

The HD3-$0.001SbI_3+Bi_2Te_{1.9}Se_{1.1}$ bulk samples have been re-prepared triple by the same procedure. The high *zT* values have been reproduced; meanwhile all the samples have an average value of *zT* ~0.9 in the temperature range from 300 K to 650 K. (Fig. 9b). Compared with other n-type med-temperature TE materials such as Mg_2Si[11], $Bi_2Te_{1.5}Se_{1.5}$[29], Bi_2Te_2S, Bi_2SeS_2[30], our work shows the best TE performance during whole temperature range, especially in the range of 500-650 K (Fig. 9c).

In previous work, our group applied hot deformation directly to commercialized $Bi_2Te_{2.79}Se_{0.21}$ ingots, whose Se content is low and suitable for use in room temperature range (300–400 K), and *zT* ~1.2 at 350K was achieved[48]. Meanwhile, we also further increased Se content and demonstrated that repetitive hot-deformed $Bi_2Te_{2.3}Se_{0.7}$ alloys show the best *zT* in the temperature range 400–500 K[21]. In this paper, we increase Se content to 1.1 and fabricate high zT HD3-$0.001SbI_3+Bi_2Te_{1.9}Se_{1.1}$ material applied in the temperature range of 500–650 K. These results demonstrate the promising application of bismuth telluride alloys for power generation (Fig. 9d).

Conclusions

In summary, we successfully shifted the maximum *zT* values of n-type bismuth telluride-based alloys to relatively high temperatures (approximately 600K) by Se-alloying and SbI_3 doping. The detrimental effects of minority carriers on the Seebeck coefficient and thermal conductivity were suppressed as a result of increases in both the band gap and electron concentration. At last, high-performance bismuth telluride-based alloys were fabricated utilizing the repetitive HD method. The Se alloying gives out a bigger band gap among all samples to suppress detrimental intrinsic conduction. A donor-like effect and SbI_3 doping increase the electron concentration simultaneous, inhabiting the ambipolar effects for higher temperature use. Aside from this, the lattice thermal conductivity was considerably reduced by the presence of recrystallization-induced in situ nanostructures and high density lattice defects. As a consequence of these factors, the HD3-$0.001SbI_3+Bi_2Te_{1.9}Se_{1.1}$ materials, showed a maximum *zT* of ~1.1 at approximately 600K and the largest average zT_{av} of 0.9 in the range of 300–650K. These data indicate significant promise for these materials in mid-temperature power generation. As these results proved extremely reproducible, this is a promising approach for the mass production of high-performance TE materials.

Acknowledgements

The work was supported by the National Basic Research Program of China (2013CB632503), the Nature Science Foundation of China (51271165 and 51171171), the Program for New Century Excellent Talents in University of China (NCET-12-0495), the Program for Innovative Research Team in University of Ministry of Education of China (IRT13037), and the PhD program Foundation of Ministry of Education of China (20120101110082).

Notes and references

1 Kim SI, Lee KH, Mun HA, Kim HS, Hwang SW, Roh JW, Science 2015;348:109-14.
2 Poudel B, Hao Q, Ma Y, Lan Y, Minnich A, Yu B, Science 2008;320:634-8.
3 Tritt TM, Science 1999;283:804-5.
4 Dresselhaus MS, Chen G, Tang MY, Yang RG, Lee H, Wang DZ, Advanced Materials 2007;19:1043-53.
5 Pei Y, Lensch-Falk J, Toberer ES, Medlin DL, Snyder GJ, Advanced Functional Materials 2011;21:241-9.
6 Biswas K, He J, Blum ID, Wu CI, Hogan TP, Seidman DN, Nature 2012;489:414-8.
7 Hsu KF, Loo S, Guo F, Chen W, Dyck JS, Uher C, Science 2004;303:818-21.
8 Xie H, Wang H, Pei Y, Fu C, Liu X, Snyder GJ, Advanced Functional Materials 2013;23:5123-30.
9 Yu C, Zhu T-J, Shi R-Z, Zhang Y, Zhao X-B, He J, Acta Materialia 2009;57:2757-64.
10 Shi X, Yang J, Salvador JR, Chi M, Cho JY, Wang H, Journal of the American Chemical Society 2011;133:7837-46.
11 Du Z, Zhu T, Chen Y, He J, Gao H, Jiang G, Journal of Materials Chemistry 2012;22:6838.
12 Liu W, Tan X, Yin K, Liu H, Tang X, Shi J, Physical Review Letters 2012;108.
13 Liu X, Zhu T, Wang H, Hu L, Xie H, Jiang G, Advanced Energy Materials 2013;3:1238-44.
14 Zhao L-D, Lo S-H, Zhang Y, Sun H, Tan G, Uher C, Nature 2014;508:373-7.
15 Hsu C-T, Huang G-Y, Chu H-S, Yu B, Yao D-J, Applied Energy 2011;88:1291-7.
16 Wu C, Applied Thermal Engineering 1996;16:63-9.
17 T. D. Barr and F. Dahlen, J. Geophys. Res., 1989, 94, 3923.
18 DiSalvo FJ, Science 1999;285:703-6.
19 Hu L, Gao H, Liu X, Xie H, Shen J, Zhu T, Journal of Materials Chemistry 2012;22:16484.
20 Hu L-P, Zhu T-J, Wang Y-G, Xie H-H, Xu Z-J, Zhao X-B, NPG Asia Materials 2014;6:e88.
21 Hu L, Zhu T, Liu X, Zhao X, Advanced Functional Materials 2014;24:5211-8.

Journal of Materials Chemistry C Accepted Manuscript

This journal is © The Royal Society of Chemistry 20xx

22 Hu LP, Liu XH, Xie HH, Shen JJ, Zhu TJ, Zhao XB, Acta Materialia 2012;60:4431-7.
23 Zhu T, Xu Z, He J, Shen J, Zhu S, Hu L, Journal of Materials Chemistry A 2013;1:11589.
24 Yan X, Poudel B, Ma Y, Liu WS, Joshi G, Wang H, Nano letters 2010;10:3373-8.
25 Shen J-J, Zhu T-J, Zhao X-B, Zhang S-N, Yang S-H, Yin Z-Z., Energy & Environmental Science 2010;3:1519-23.
26 Li J, Tan Q, Li J-F, Liu D-W, Li F, Li Z-Y, Advanced Functional Materials 2013;23:4317-23.
27 Mehta RJ, Zhang Y, Zhu H, Parker DS, Belley M, Singh DJ, Nano letters 2012;12:4523-9.
28 Zhao LD, Zhang BP, Li JF, Zhang HL, Liu WS, Solid State Sciences 2008;10:651-8.
29 Wang S, Tan G, Xie W, Zheng G, Li H, Yang J, Journal of Materials Chemistry 2012;22:20943.
30 Liu W, Lukas KC, McEnaney K, Lee S, Zhang Q, Opeil CP, Energy Environ Sci 2013;6:552-60.
31 Hu LP, Zhu TJ, Yue XQ, Liu XH, Wang YG, Xu ZJ, Acta Materialia 2015;85:270-8.
32 Imamuddin M, Dupre A, physica status solidi (a) 1972;10:415-24.
33 Teramoto I, Takayanagi S, J Phys Chem Solids 1961;19:124-9.
34 Delves R, Bowley A, Hazelden D, Goldsmid H, Proceedings of the Physical Society 1961;78:838.
35 Xie W, He J, Zhu S, Holgate T, Wang S, Tang X, Journal of Materials Research 2011;26:1791-9.
36 Lotgering FK, Journal of Inorganic and Nuclear Chemistry 1959;9:113-23.
37 Shen JJ, Hu LP, Zhu TJ, Zhao XB, Applied Physics Letters 2011;99:124102.
38 Ben-Yehuda O, Shuker R, Gelbstein Y, Dashevsky Z, Dariel MP, Journal of Applied Physics 2007;101:113707.
39 Birkholz U, Astrophysik Physik Und Physikalische Chemie 1958;13:780-92.
40 Jiang J, Chen L, Bai S, Yao Q, Wang Q, Scripta materialia 2005;52:347-51.
41 Navrátil J, Starý Z, Plecháček T, Materials Research Bulletin 1996;31:1559-66.
42 West D, Sun YY, Wang H, Bang J, Zhang SB, Physical Review B 2012;86.
43 Stary Z, Horak J, Stordeur M, Stolzer M, J Phys Chem Solids 1988;49:29-34.
44 I. G. Austin and A. Sheard, J. Electron. Control 1957;3, 236.
45 M. J. Smith, E. S. Kirk, and C. W. Spencer, J. Appl. Phys.1960; 31, 1504 .
46 [46] Miller GR, Li C-Y, Spencer CW, Journal of Applied Physics 1963;34:1398.
47 J. Black, E. Conwell, L. Seigle, and C. W. Spencer, J. Phys. Chem. Solids 1957;2, 240.
48 Drabble JR, Goodman CH, J Phys Chem Solids 1958;5:142-4.

Journal of Materials Chemistry C Accepted Manuscript

Journal of Materials Chemistry C - TC-ART-07-2015-002263
Title: "High performance n-type bismuth telluride based alloys for mid-temperature power generation" by Zhenglong Tang, Lipeng Hu, and Tiejun Zhu, Xiaohua Liu, Xinbing Zhao.

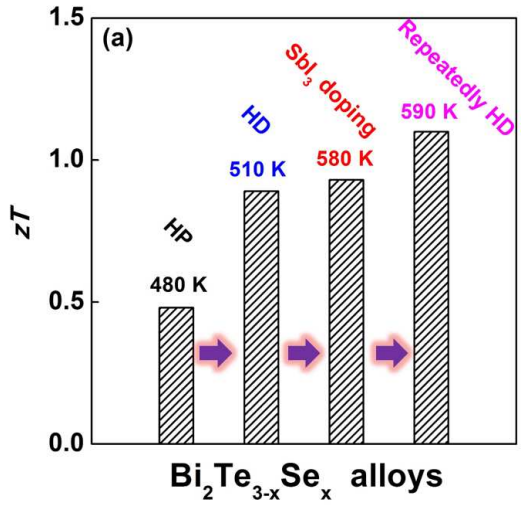

We combine Se alloying, SbI_3 doping and repeated hot deformation to obtain high-performance n-type Bi_2Te_3 based med-temperature thermoelectric materials for power generation.

Journal of Materials Chemistry C Accepted Manuscript